Communications in Analysis and Mechanics

https://www.aimspress.com/journal/cam

Communications in Analysis and Mechanics, 18(1): 208–227.
DOI: 10.3934/cam.2026008
Received: 24 July 2025
Revised: 09 November 2025
Accepted: 04 January 2026
Published: 13 March 2026

Research article

Investigation of chaotic behavior in a Lorenz-like system with fractional derivatives

Seda İĞRET ARAZ[1] **and Mehmet Akif ÇETİN**[2,*]

[1] Siirt University, Department of Mathematics Education, Siirt, Turkey

[2] ALTSO Vocational School, Alanya Alaaddin Keykubat University, Antalya, Turkey

* **Correspondence:** Email: akif.cetin@alanya.edu.tr.

Abstract: In recent years, fractional-order dynamical systems have attracted significant attention because of their ability to describe memory effects and hereditary properties found in many physical and engineering processes. Fractional calculus extends the concept of differentiation and integration to non-integer orders, providing a more flexible mathematical framework for modeling and analyzing complex system behaviors. Within this framework, the study of chaotic dynamics in fractional-order systems has become an active research area since many well-known chaotic models show new and qualitatively different behaviors when generalized to fractional derivatives. This study revisits a classical chaotic system originally defined in the integer-order setting and analyzes its behavior using fractional-order calculus. The main objective is to examine how fractional differentiation influences the system's chaotic dynamics and sensitivity to initial conditions. To achieve this, numerical simulations are performed to demonstrate the effects of different fractional orders on the development and evolution of chaotic behavior.

Keywords: fractional-order chaotic systems; nonlinear dynamics; memory effects; numerical simulation
Mathematics Subject Classification: 34C28, 70Kxx, 35A35

1. Introduction

In recent decades, the study of nonlinear dynamical systems has significantly changed our understanding of deterministic models, showing how even simple systems can evolve in complex and unpredictable ways. This phenomenon, known as chaos theory, has influenced many areas of science and engineering, including physics, meteorology, biology, and control theory. A key example is the class of Lorenz-like systems, which are deterministic in definition but highly sensitive to initial conditions, a fundamental property of chaotic dynamics.

The origins of chaos theory go back to the work of Edward Lorenz [1], who showed with a simplified model of atmospheric convection that deterministic systems could produce non-periodic and seemingly long-time behavior. The Lorenz system revealed what became known as a strange attractor, a complex geometric structure in phase space that represents chaotic motion. This discovery challenged traditional ideas of predictability and opened new directions in the study of nonlinear systems.

Later, Sparrow [2] carried out a detailed mathematical study of the Lorenz equations, focusing on bifurcations and attractor structures. His work helped establish the mathematical foundation for describing chaotic behavior. Other researchers proposed similar systems with related structures. For example, Chen and Ueta introduced the Chen system, which differs from the Lorenz system but still shows chaotic behavior with its own attractor geometry [3]. Later, Lü et al. proposed the Lü system, which connects the Lorenz and Chen systems through changes in a key parameter [4].

These Lorenz-like systems are now widely used as models of chaos, both for theoretical studies and for practical applications, such as circuit design, secure communication, and cryptography. Their study continues to reveal the deep links between nonlinearity, determinism, and unpredictability in dynamical systems.

Research on fractional-order chaotic systems has also grown rapidly. In [3], Chen and Ueta introduced the Chen system, which became an important basis for later fractional-order studies. In [5], Li and Chen then examined a fractional version of this system, showing how fractional derivatives affect the onset and evolution of chaos, and suggesting control methods suited for fractional dynamics. Petráš [6] provided a broad overview of fractional-order nonlinear systems, covering modeling, analysis, and simulation methods. Tavazoei and Haeri [7] made a key theoretical contribution by proving that linear fractional-order systems cannot produce chaos, emphasizing the role of nonlinearity. Odibat et al. [8] extended these ideas by studying fractional versions of the Chen, Rössler, and Chua systems, showing how fractional differentiation changes system dynamics and stability. Together, these studies demonstrate how fractional calculus enriches the study of classical chaotic systems, offering new insights and modeling possibilities [9–14].

More recently, the chaotic system considered in [15] has been studied for its complex dynamics and sensitivity to initial conditions. However, many real-world systems display memory effects that cannot be captured well by classical models. Fractional-order calculus, which generalizes derivatives to non-integer orders, offers a powerful framework for capturing memory and hereditary properties of complex dynamical systems—features that classical integer-order models often fail to represent accurately. Motivated by this, the present study modifies the Lorenz-like system introduced in [15] using two distinct fractional operators: the Caputo and Caputo–Fabrizio derivatives. This dual approach not only broadens the analytical scope of the model but also enables a comparative investigation of how different types of fractional derivatives influence the system's dynamics.

By embedding the system within a fractional-order framework, the study aims to examine the impact of fractional differentiation on chaotic behavior, especially in terms of sensitivity to initial conditions and system parameters. Numerical simulations demonstrate that the system's chaotic features persist under fractionalization but may exhibit qualitatively different dynamics depending on the fractional order and kernel type. This contributes meaningfully to the growing body of research on fractional-order chaotic systems and highlights the potential of non-integer-order modeling in capturing wider dynamical behaviors than their classical frameworks.

Now, we provide some definitions of fractional derivatives with power law, and exponential decay kernels.

The Caputo-Fabrizio fractional derivative [16] of the function $\omega(t) \in H^1(0,T)$ is given by

$$ {}_0^{CF}D_t^{\alpha}\omega(t) = \frac{1}{1-\alpha}\int_0^t \omega'(\zeta)\exp\left[-\frac{\alpha}{1-\alpha}(t-\zeta)\right]d\zeta, \tag{1.1} $$

where $0 < \alpha < 1$ and $H^1(0,T)$ describes the Hilbert space. The associated integral is defined by

$$ {}_0^{CF}J_t^{\alpha}\omega(t) = (1-\alpha)\omega(t) + \alpha\int_0^t \omega(\zeta)\,d\zeta. \tag{1.2} $$

The Caputo fractional derivative [17] of the function $\omega(t) \in H^1(0,T)$ is defined by

$$ {}_0^{C}D_t^{\alpha}\omega(t) = \frac{1}{\Gamma(1-\alpha)}\int_0^t \omega'(\zeta)(t-\zeta)^{-\alpha}\,d\zeta, \tag{1.3} $$

where $0 < \alpha \leq 1$.

2. Some analysis, including existence, uniqueness, and chaotic dynamics

The analysis of initial value problems in ordinary differential equations fundamentally relies on the existence and uniqueness of solutions to ensure that the model under consideration is well-posed. Without such guarantees, the predictive power and internal consistency of the mathematical formulation would be compromised. To establish these properties, this work employs the Picard iteration method, a constructive approach based on successive approximations that converges under appropriate conditions. In particular, the proof is based on verifying two key hypotheses: the Lipschitz continuity of the function with respect to the dependent variable and the linear growth condition. The Lipschitz condition ensures the contraction property necessary for the convergence of the iterative sequence to a unique fixed point, while the linear growth condition guarantees the boundedness and continuity required for existence over a finite interval. These conditions, once satisfied, confirm both the existence and uniqueness of solutions, thereby validating the formulation of the differential system. The absence of any existence and uniqueness analysis for the classical version of the chaotic system addressed in this study, as noted in [15], necessitates conducting such an analysis. Therefore, in this section, we aim to investigate the conditions under which the associated chaotic system satisfies the criteria presented above, prove the existence and uniqueness of its solution, and present aspects of chaotic theory, including the bifurcation diagram, Lyapunov exponents, and fractal dimension. The chaotic system [15] we focus on is presented below:

$$ \begin{aligned} x'(t) &= \sigma_1 y - \sigma x + d\sin z \\ y'(t) &= x(\rho - z) - y + eyz \\ z'(t) &= xy - \beta z + \gamma\cos x. \end{aligned} \tag{2.1} $$

The Lorenz-like system exhibits chaotic behaviors with following parameters:

$$ \sigma_1 = 3.8; \sigma = 3.5; \rho = 1; \beta = 1.3; d = 1; e = 0.5; \gamma = 30.5, \tag{2.2} $$

and initial conditions

$$x(0) = 0.1; y(0) = 0.1; z(0) = 8. \tag{2.3}$$

Equilibrium point is calculated as $(1.6266, 1.3885, 0.4298)$.

As performed in [15], we present the eigenvalues of the Jacobian matrix based on the parameters and equilibrium point defined above:

$$\lambda_{1,2} = -3.6368 \pm 5.7240i, \lambda_3 = 1.6884. \tag{2.4}$$

We know that a positive eigenvalue makes the equilibrium locally unstable, while the negative complex pair causes spiral convergence. This saddle-focus structure suggests potential for chaos, but confirming chaos requires further tests, such as Lyapunov exponents, phase portraits, and Kaplan–Yorke dimension. As specified in [15], Lyapunov exponents are found by using Wolf algorithm [18] as follows:

$$\lambda_1 = 3.1761, \lambda_2 = 0.000, \lambda_3 = -2.2103. \tag{2.5}$$

The representation related to Lyapunov exponents is presented in Figure 1.

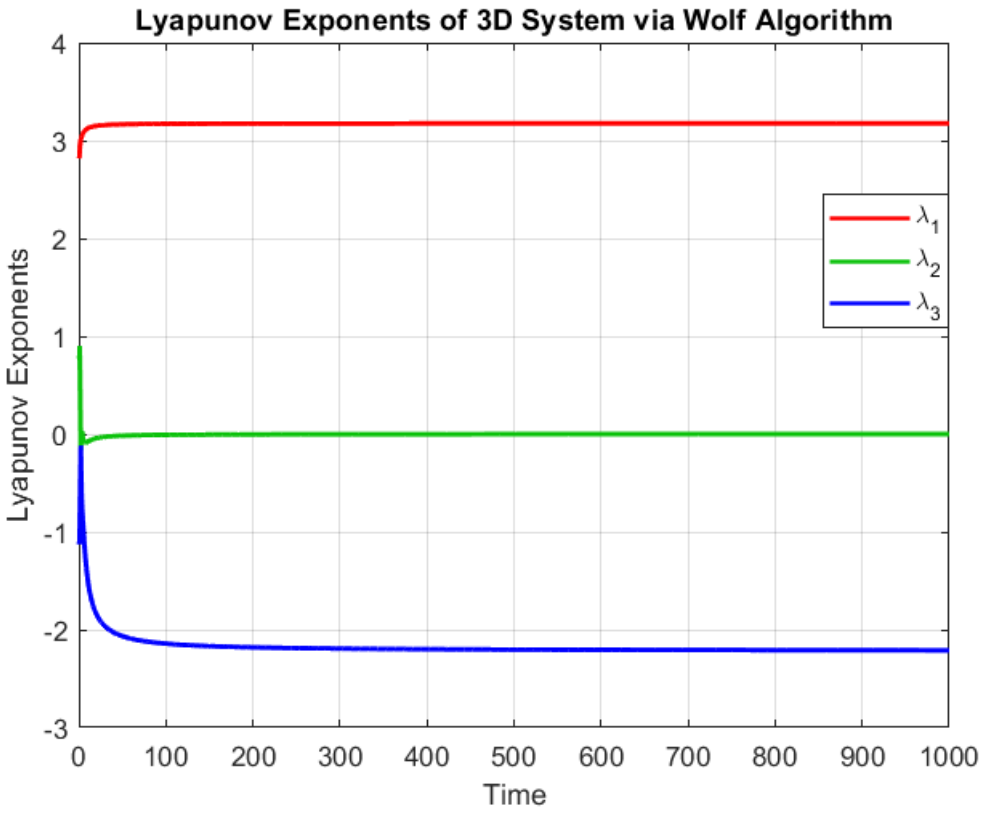

Figure 1. Time evolution of the three Lyapunov exponents ($\lambda_1 > 0, \lambda_2 = 0, \lambda_3 < 0$) of the proposed chaotic system.

Figure 1 demonstrates that the largest Lyapunov exponent ($\lambda_1 > 0$) remains positive over time, indicating sensitivity to initial conditions and confirming the presence of chaos. Kaplan-Yorke dimension [19] of the system [15] is found as:

$$D_{KY} = 2 + \frac{3.1761 + 0.000}{|-2.2103|} \approx 2 + 1.437 = 3.437. \tag{2.6}$$

This result confirms the presence of a non-integer dimension, characteristic of a strange attractor. To gain deeper insight into the system's structure and nonlinear properties, a detailed qualitative analysis is presented in the subsequent section.

Bifurcation analysis and the largest Lyapunov exponent

Bifurcation analysis examines how a system's dynamics change qualitatively as a control parameter is varied. It highlights transitions such as the onset of periodic oscillations, period-doubling, and the emergence of chaos. This method also provides valuable insights into the stability and complexity of nonlinear dynamical systems. For the problem considered here, the bifurcation diagram is shown in Figure 2.

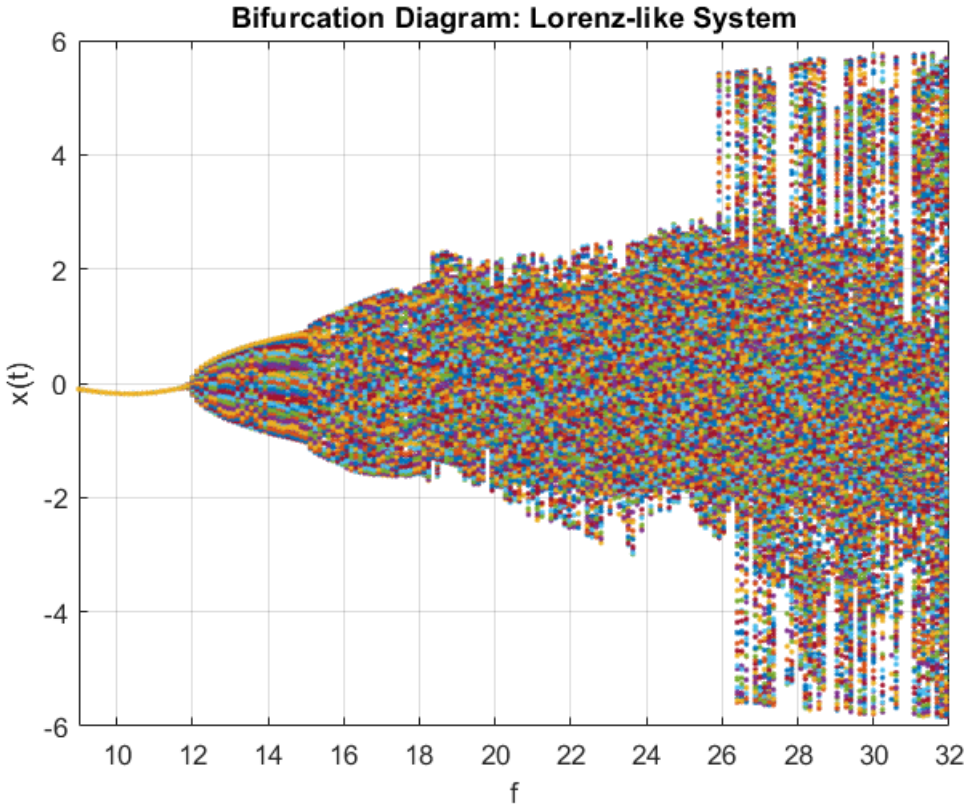

Figure 2. The bifurcation diagram of the Lorenz-like chaotic model with $\gamma \in [9, 35]$, $\sigma_1 = 3.8; \sigma = 3.5; \rho = 1; \beta = 1.3; d = 1; e = 0.5$.

In Figure 2, we simulate the graphical representation of the bifurcation diagram for proposed system with $\gamma \in [9, 35], \sigma_1 = 3.8; \sigma = 3.5; \rho = 1; \beta = 1.3; d = 1; e = 0.5$. At low values of $\gamma \in [5, 10]$, the system remains in a stable equilibrium without oscillations. When $\gamma \in [10, 13]$, the first bifurcation occurs and periodic oscillations appear, forming a limit cycle. For $\gamma \in [13, 20]$, period-doubling takes place, leading to increasingly complex dynamics. Beyond $\gamma > 20$, the system

enters a chaotic regime, showing irregular trajectories and sensitivity to initial conditions, confirmed by positive Lyapunov exponents.

Existence and uniqueness of the system

To demonstrate the existence of the above system's solution we will use the Picard iteration. We consider the following Cauchy problem:

$$\begin{cases} F'(t) = f_i(t, F(t)), & \text{if } t \in [0, T] \\ F(t_0) = F^0, \end{cases} . \tag{2.7}$$

Here, we denote

$$F(t) = \begin{bmatrix} x(t) \\ y(t) \\ z(t) \end{bmatrix}. \tag{2.8}$$

to avoid complexity. $f_i : I \times \mathbb{R} \to \mathbb{R}, i = 1, .., 3$ is assumed to be Lipschitz and bounded [20]. We wish to prove that above equation has a unique solution. Using the Picard iteration, we have

$$F_{n+1}(t) = F(t_0) + \int_{t_0}^{t} f_i(s, F_n(s))\, ds, \text{ if } t \in [0, T], \tag{2.9}$$

and

$$F_n(t) = F(t_0) + \int_{t_0}^{t} f_i(s, F_{n-1}(s))\, ds, \text{ if } t \in [0, T]. \tag{2.10}$$

We now evaluate

$$|F_{n+1}(t) - F_n(t)| \leq \int_{t_0}^{t} |f_i(s, F_n(s)) - f_i(s, F_{n-1}(s))|\, ds, \text{ if } t \in [0, T]. \tag{2.11}$$

With the help of Lipschitz condition of f, we get

$$\begin{aligned} |F_{n+1}(t) - F_n(t)| &\leq L \int_{t_0}^{t} |F_n(s) - F_{n-1}(s)|\, ds, \text{ if } t \in [0, T] \\ &\leq L \int_{t_0}^{t} |F_n(s) - F_{n-1}(s)|\, ds \\ &\leq L \left| \left\{ \int_{t_0}^{\tau} |(f_i(l, F_{n-1}) - f_i(l, F_{n-2}))| \right\} dl \right| ds, \text{ if } t \in [0, T] \\ &\leq L^n \int_{t_0}^{t} \int_{t_0}^{\tau} \ldots \int_{t_0}^{\lambda} |F_1 - F_0|\, d\lambda \ldots ds \\ &\leq L^n M \frac{(t - t_0)^n}{n!} \end{aligned} \tag{2.12}$$

where $L > 0$. Thus, we get

$$|F_{n+1}(t) - F_n(t)| \leq L^n M \frac{(t - t_0)^n}{n!}. \tag{2.13}$$

If F_i is a contraction, then

$$\lim_{n \to \infty} |F_{n+1}(t) - F_n(t)| = 0, \tag{2.14}$$

which guarantees the existence of solution.

Theorem: Assume that there exists positive constants k_i, $\bar{k}_i$ such that
(i) $\forall i \in \{1,2,3\}$

$$\left|F_i\left(x_i,t\right)-F_i\left(x_i',t\right)\right|^2 \leq k_i\left|x_i-x_i'\right|^2,$$

(ii) $\forall\,(x,t)\in R^3\times[0,T]$

$$\left|F_i\left(x_i,t\right)\right|^2 \leq \bar{k}_i\left(1+\left|x_i\right|^2\right).$$

Proof. Before starting with the proof, we shall first define the following norm:

$$\|\psi\|_\infty = \sup_{0\leq t\leq T}\left|\psi\left(t\right)\right|.$$

We start with the function $F_1\left(t,\varphi\right)$. Then, we will show that

$$\begin{aligned}\left|F_1\left(x_1,t\right)-F_1\left(x_2,t\right)\right|^2 &= \left|-\sigma\left(x_1-x_2\right)\right|^2\\ &\leq \left(\sigma^2+\varepsilon_1\right)\left|x_1-x_2\right|^2\\ &\leq k_1\left|x_1-x_2\right|^2,\end{aligned}$$

where $k_1=\sigma^2+\varepsilon_1$. Then, we write

$$\begin{aligned}\left|F_2\left(y_1,t\right)-F_2\left(y_2,t\right)\right|^2 &= \left|\left(ez-1\right)\left(y_1-y_2\right)\right|^2\\ &\leq 2\left|e^2\left|z\right|^2+1\right|\left|y_1-y_2\right|^2\\ &\leq 2\left|e^2\sup_{0\leq t\leq T}\left|z\right|^2+1\right|\left|y_1-y_2\right|^2\\ &\leq 2\left|e^2\left\|z\right\|_\infty^2+1\right|\left|y_1-y_2\right|^2\\ &\leq k_2\left|y_1-y_2\right|^2,\end{aligned}$$

where $k_2=2\left|e^2\left\|z\right\|_\infty^2+1\right|$. Next, we write

$$\begin{aligned}\left|F_3\left(z_1,t\right)-F_3\left(z_2,t\right)\right|^2 &= \left|-\beta\left(z_1-z_2\right)\right|^2\\ &\leq \left(\beta^2+\varepsilon_2\right)\left|z_1-z_2\right|^2\\ &\leq k_3\left|z_1-z_2\right|^2,\end{aligned}$$

where $k_3=\beta^2+\varepsilon_2$. We verified the first condition for all functions. To verify the second condition for all functions, we write the following:

$$\begin{aligned}\left|F_1\left(x,t\right)\right|^2 &= \left|\sigma_1 y-\sigma x+d\sin z\right|^2\\ &\leq 3\left[\sigma_1^2\left|y\right|^2+\sigma^2\left|x\right|^2+d^2\right]\\ &\leq 3\left[\sigma_1^2\sup_{0\leq t\leq T}\left|y\right|^2+\sigma^2\left|x\right|^2+d^2\right]\\ &\leq 3\left[\sigma_1^2\left\|y\right\|_\infty^2+\sigma^2\left|x\right|^2+d^2\right]\\ &\leq 3\left[\sigma_1^2\left\|y\right\|_\infty^2+d^2\right]\left[1+m_1\left|x\right|^2\right]\\ &\leq \bar{k}_1\left(1+\left|x\right|^2\right),\end{aligned}$$

under the condition $m_1 = \frac{\sigma^2}{\sigma_1^2\|y\|_\infty^2+d^2} < 1$. Later,

$$\begin{aligned}
|F_2(y,t)|^2 &= |x(\rho-z)-y+eyz|^2 \\
&\leq 3\left(|x|^2(\rho-z)^2+|y|^2+e^2|y|^2|z|^2\right) \\
&\leq 3\left(2|x|^2\rho^2+2|x|^2|z|^2+|y|^2+e^2|y|^2|z|^2\right) \\
&\leq 3\left(2\rho^2\sup_{0\leq t\leq T}|x|^2+2\sup_{0\leq t\leq T}|x|^2\sup_{0\leq t\leq T}|z|^2+|y|^2+e^2|y|^2\sup_{0\leq t\leq T}|z|^2\right) \\
&\leq 3\left(2\rho^2\|x\|_\infty^2+2\|x\|_\infty^2\|z\|_\infty^2+\left(1+e^2\|z\|_\infty^2\right)|y|^2\right) \\
&\leq 3\left(2\rho^2\|x\|_\infty^2+2\|x\|_\infty^2\|z\|_\infty^2\right)\left(1+m_2|y|^2\right) \\
&\leq \bar{k}_2\left(1+|y|^2\right),
\end{aligned}$$

under the condition $m_2 = \frac{1+e^2\|z\|_\infty^2}{2\rho^2\|x\|_\infty^2+2\|x\|_\infty^2\|z\|_\infty^2} < 1$. Finally, we have

$$\begin{aligned}
|F_3(z,t)|^2 &= |xy-\beta z+\gamma\cos x|^2 \\
&\leq 3\left(|x|^2|y|^2+\beta^2|z|^2+\gamma^2\right) \\
&\leq 3\left(\sup_{0\leq t\leq T}|x|^2\sup_{0\leq t\leq T}|y|^2+\beta^2|z|^2+\gamma^2\right) \\
&\leq 3\left(\|x\|_\infty^2\|y\|_\infty^2+\gamma^2\right)\left(1+m_3|z|^2\right) \\
&\leq \bar{k}_3\left(1+|z|^2\right),
\end{aligned}$$

under the condition $m_3 = \frac{\beta^2}{\|x\|_\infty^2\|y\|_\infty^2+\gamma^2} < 1$. Thus, it is proven that the solution of the considered chaotic system is unique when

$$\max\{m_1, m_2, m_3\} < 1.$$

3. Numerical scheme for Lorenz-like attractor

In this section, we construct a numerical scheme with Lagrange interpolation polynomial [21, 22] and L1 method [23, 24] for fractional order Lorenz-like chaotic system with Caputo-Fabrizio and Caputo fractional derivatives. It is worth emphasizing that the accuracies of the associated methods are thoroughly analyzed in [21] and [22], respectively. To acquire this, firstly we consider the following attractor:

$$\begin{aligned}
{}_0^{CF}D_t^\alpha x(t) &= \sigma_1 y-\sigma x+d\sin z \\
{}_0^{CF}D_t^\alpha y(t) &= x(\rho-z)-y+eyz \\
{}_0^{CF}D_t^\alpha z(t) &= xy-\beta z+\gamma\cos x.
\end{aligned} \tag{3.1}$$

We can facilitate the above system as

$$\begin{aligned}
{}_0^{CF}D_t^\alpha x(t) &= a(x,y,z,t) \\
{}_0^{CF}D_t^\alpha y(t) &= b(x,y,z,t)
\end{aligned} \tag{3.2}$$

$$ {}_{0}^{CF}D_{t}^{\alpha} z(t) = c(x,y,z,t), $$

where

$$ \begin{aligned} a(x,y,z,t) &= \sigma_1 y - \sigma x + d\sin z \\ b(x,y,z,t) &= x(\rho - z) - y + eyz \\ c(x,y,z,t) &= xy - \beta z + \gamma\cos x. \end{aligned} $$

Before proceeding with the scheme, we denote the following notations to avoid complexity

$$ \mathbf{u}(t) = \begin{bmatrix} x(t) \\ y(t) \\ z(t) \end{bmatrix}, \mathbf{F}(t,\mathbf{u}(t)) = \begin{bmatrix} a(x,y,z,t) \\ b(x,y,z,t) \\ c(x,y,z,t) \end{bmatrix}. $$

We modify our model as follows:

$$ {}_{0}^{CF}D_{t}^{\alpha}\mathbf{u}(t) = \mathbf{F}(t,\mathbf{u}(t)). $$

Then, applying the Caputo-Fabrizio integral we obtain the following:

$$ \mathbf{u}(t) = \mathbf{u}_0 + (1-\alpha)\mathbf{F}(t,\mathbf{u}(t)) + \alpha\int_0^t \mathbf{F}(\tau,\mathbf{u}(\tau))\,d\tau. $$

After this we rewrite the above system, at $t = t_{n+1}$

$$ \mathbf{u}(t_{n+1}) = \mathbf{u}_0 + (1-\alpha)\mathbf{F}\left(t_{n+1},\mathbf{u}^{n+1}\right) + \alpha\int_0^{t_{n+1}} \mathbf{F}(\tau,\mathbf{u}(\tau))\,d\tau, \tag{3.3} $$

and at $t = t_n$

$$ \mathbf{u}(t_n) = \mathbf{u}_0 + (1-\alpha)\mathbf{F}(t_n,\mathbf{u}^n) + \alpha\int_0^{t_n} \mathbf{F}(\tau,\mathbf{u}(\tau))\,d\tau. \tag{3.4} $$

Taking the difference of (3.3) and (3.4), we reach the following:

$$ \begin{aligned} \mathbf{u}(t_{n+1}) &= \mathbf{u}(t_n) + (1-\alpha)\left[\mathbf{F}(t_n,\mathbf{u}^n) - \mathbf{F}\left(t_{n-1},\mathbf{u}^{n-1}\right)\right] \\ &\quad + \alpha\int_{t_n}^{t_{n+1}} \mathbf{F}(\tau,\mathbf{u}(\tau))\,d\tau. \end{aligned} $$

If we replace the function $\mathbf{F}(\tau,\mathbf{u}(\tau))$ by their Lagrange interpolation polynomials, we get the following:

$$ \begin{aligned} \mathbf{u}(t_{n+1}) &= \mathbf{u}(t_n) + (1-\alpha)\left[\mathbf{F}(t_n,\mathbf{u}^n) - \mathbf{F}\left(t_{n-1},\mathbf{u}^{n-1}\right)\right] \\ &\quad + \alpha\left[\frac{\mathbf{F}(t_n,\mathbf{u}^n)}{h}\int_{t_n}^{t_{n+1}} (\tau - t_{n-1})\,d\tau - \frac{\mathbf{F}\left(t_{n-1},\mathbf{u}^{n-1}\right)}{h}\int_{t_n}^{t_{n+1}} (\tau - t_n)\,d\tau\right], \end{aligned} $$

where

$$\int_{t_n}^{t_{n+1}} (\tau - t_{n-1})\, d\tau = \frac{3h^2}{2},$$

$$\int_{t_n}^{t_{n+1}} (\tau - t_n)\, d\tau = \frac{h^2}{2}.$$

Then, we have

$$\begin{aligned} \mathbf{u}(t_{n+1}) &= \mathbf{u}(t_n) + (1-\alpha)\left[\mathbf{F}(t_n, \mathbf{u}^n) - \mathbf{F}\left(t_{n-1}, \mathbf{u}^{n-1}\right)\right] \\ &\quad +\alpha\left[\frac{3h}{2}\mathbf{F}(t_n, \mathbf{u}^n) - \frac{h}{2}\mathbf{F}\left(t_{n-1}, \mathbf{u}^{n-1}\right)\right]. \end{aligned}$$

Now, the numerical algorithm [23, 24] will be presented for fractional order Lorenz-like chaotic system with Caputo fractional derivative which is given by

$$\begin{cases} {}_{t_0}^{C}D_t^{\alpha}\mathbf{u}(t) = \mathbf{F}(t_k, \mathbf{u}(t_k)) \\ \mathbf{u}(0) = \mathbf{u}_0 \end{cases}.$$

For discretization, the domain $[t_0, T]$ is isometrically divided into $k+1$ parts denoted by $t_0, t_1, ..., t_k = T$ with step size $h = \frac{T-t_0}{k+1}$. Then, the derivative of $\mathbf{u}$ at $t = t_k$ is given by the following:

$$\begin{aligned} {}_{t_0}^{C}D_t^{\alpha}\mathbf{u}(t)\big|_{t=t_k} &= \frac{1}{\Gamma(1-\alpha)}\int_{t_0}^{t_k} (t_k - s)^{-\alpha}\,\mathbf{u}'(s)\, ds \\ &= \frac{1}{\Gamma(1-\alpha)}\sum_{j=1}^{k}\int_{t_{j-1}}^{t_j} (t_k - s)^{-\alpha}\,\mathbf{u}'(s)\, ds. \end{aligned}$$

From the linear splines, we have the following:

$$\left(\Pi_{1,j}\mathbf{u}(s)\right)' = \frac{\mathbf{u}\left(t_j\right) - \mathbf{u}\left(t_{j-1}\right)}{t_j - t_{j-1}}.$$

Then, we have

$$\begin{aligned} {}_{t_0}^{C}D_t^{\alpha}\mathbf{u}(t)\big|_{t=t_k} &= \frac{1}{\Gamma(1-\alpha)}\sum_{j=1}^{k}\frac{\mathbf{u}\left(t_j\right) - \mathbf{u}\left(t_{j-1}\right)}{t_j - t_{j-1}}\left(\frac{\left(t_k - t_j\right)^{1-\alpha}}{1-\alpha} - \frac{\left(t_k - t_{j-1}\right)^{1-\alpha}}{1-\alpha}\right) \\ &= \frac{1}{\Gamma(2-\alpha)}\sum_{j=1}^{k}\frac{\mathbf{u}\left(t_j\right) - \mathbf{u}\left(t_{j-1}\right)}{t_j - t_{j-1}}\left(\left(t_k - t_j\right)^{1-\alpha} - \left(t_k - t_{j-1}\right)^{1-\alpha}\right) \\ &= \frac{1}{\Gamma(2-\alpha)}\left\{\mathbf{u}(t_0)\,A_{k,0} + \sum_{j=1}^{k-1} A_{k,j}\mathbf{u}\left(t_j\right) + A_{k,k}\mathbf{u}(t_k)\right\}, \end{aligned}$$

where

$$A_{k,j}=\begin{cases}\frac{(t_k-t_1)^{1-\alpha}-(t_k-t_0)^{1-\alpha}}{t_1-t_0}, & j=0,\\ \frac{\left(t_k-t_{j-1}\right)^{1-\alpha}-\left(t_k-t_j\right)^{1-\alpha}}{t_j-t_{j-1}}\\ -\frac{\left(t_k-t_j\right)^{1-\alpha}-\left(t_k-t_{j+1}\right)^{1-\alpha}}{t_{j+1}-t_j}, & j=1,...,k-1,\\ (t_k-t_{k-1})^{\alpha}, & j=k\end{cases}.$$

This approximation is denoted using the symbol $D^{\alpha}\mathbf{u}(t)$. Now, using this discretization in the differential equation given in equation 3.1 the following is obtained:

$$\mathbf{F}(t_k,\mathbf{u}(t_k))=\frac{1}{\Gamma(2-\alpha)}\left\{\mathbf{u}(t_0)A_{k,0}+\sum_{j=1}^{k-1}A_{k,j}\mathbf{u}\left(t_j\right)+A_{k,k}\mathbf{u}(t_k)\right\},$$

and

$$\mathbf{u}(t_k)=\frac{\Gamma(2-\alpha)\mathbf{F}(t_k,\mathbf{u}(t_k))}{A_{k,k}}-\frac{\mathbf{u}(t_0)A_{k,0}}{A_{k,k}}-\sum_{j=1}^{k-1}\frac{A_{k,j}}{A_{k,k}}\mathbf{u}\left(t_j\right).$$

For convenience, the following variables are introduced:

$$a_{k,j}=\begin{cases}\left(\frac{(t_k-t_0)^{1-\alpha}-(t_k-t_1)^{1-\alpha}}{t_1-t_0}\right)(t_k-t_{k-1})^{\alpha}, & j=0,\\ \left(\frac{\left(t_k-t_j\right)^{1-\alpha}-\left(t_k-t_{j-1}\right)^{1-\alpha}}{t_j-t_{j-1}}\right)(t_k-t_{k-1})^{\alpha}, & j=1,...,k-1\end{cases}.$$

Then, we obtain the expression

$$\begin{aligned}\mathbf{u}(t_k) &= a_{k,0}\mathbf{u}(t_0)+\sum_{j=1}^{k-1}\left(a_{k,j}-a_{k,j+1}\right)\mathbf{u}\left(t_j\right)\\ &\quad+\Gamma(2-\alpha)\frac{\mathbf{F}(t_k,\mathbf{u}(t_k))}{A_{k,k}}.\end{aligned}$$

4. Numerical Simulations

To examine the influence of the derivative order on the system's dynamic behavior, we conduct numerical simulations for various fractional-order derivatives of the chaotic system in this section. Fractional-order calculus, by incorporating memory effects, offers a more generalized and accurate framework for modeling complex dynamical systems compared to classical integer-order approaches. Investigating the system under different fractional orders allows for a comprehensive analysis of sensitivity to initial conditions, parameters, and the emergence of chaotic dynamics. These simulations are essential for understanding how fractional dynamics modify the qualitative and quantitative behavior of the system, thereby contributing to the development of more robust and realistic models for phenomena characterized by inherent chaoticity.

We choose $\alpha=0.99$ for the system

$$\begin{aligned}{}_0^{CF}D_t^{\alpha}x(t) &= \sigma_1 y-\sigma x+d\sin z \qquad (4.1)\end{aligned}$$

$$
\begin{aligned}
{}_0^{CF}D_t^{\alpha} y(t) &= x(\rho - z) - y + eyz \\
{}_0^{CF}D_t^{\alpha} z(t) &= xy - \beta z + \gamma \cos x,
\end{aligned}
$$

which has chaotic behavior with the parameters

$$
\begin{aligned}
\sigma &= 3.5;\ \sigma_1 = 3.8;\ \rho = 1.1;\ \beta = 1;\ d = 1; \\
e &= 0.48;\ \gamma = 32.05,
\end{aligned}
$$

and the initial conditions

$$x(0) = 1;\ y(0) = 1;\ z(0) = 1.$$

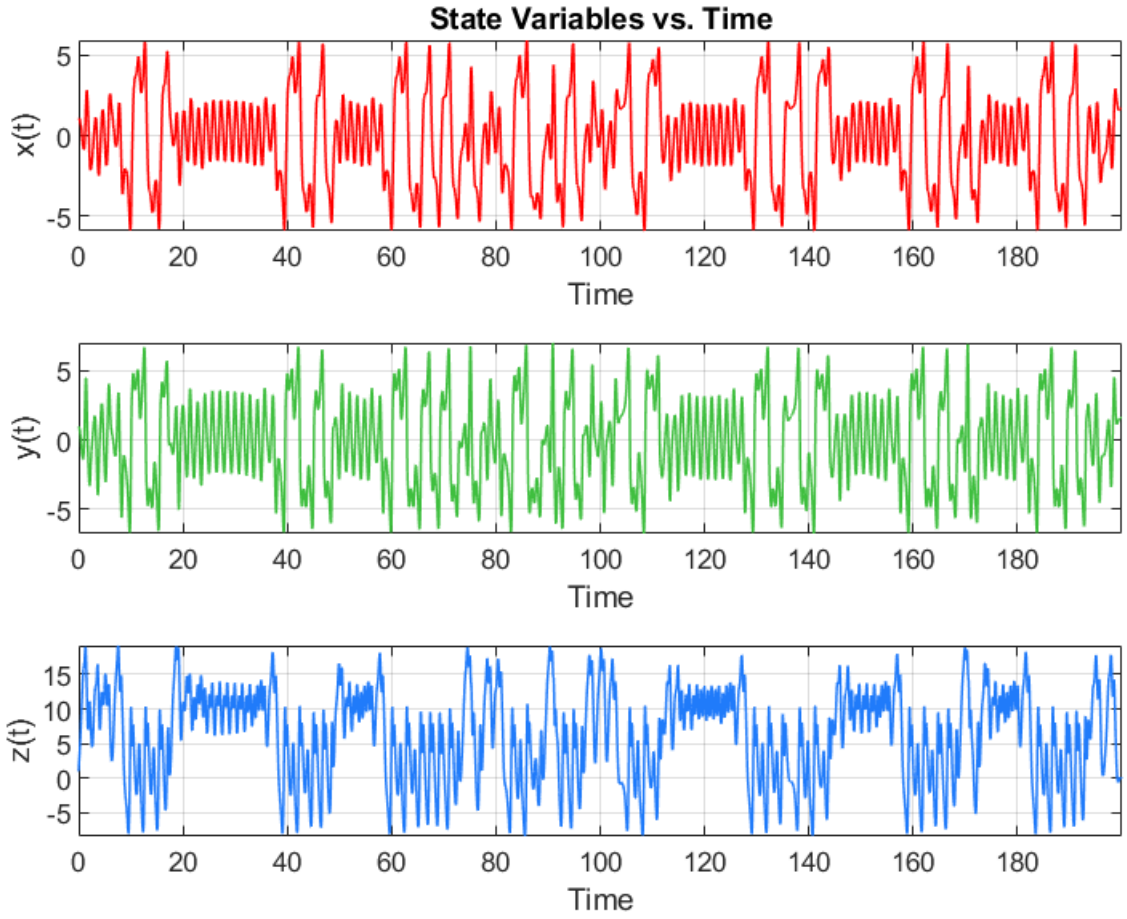

Figure 3. Time evolution of the state variables $x(t), y(t)$ and $z(t)$ of the Lorenz-like chaotic system with Caputo-Fabrizio fractional derivative.

Figure 3 presents the time evolution of the system's three state variables $x(t)$, $y(t)$, and $z(t)$. Each variable exhibits irregular, non-repeating oscillations, characteristic of chaotic systems. The amplitude of $z(t)$ is notably larger than that of $x(t)$ and $y(t)$, suggesting a more dominant or energetic role in

the system dynamics. The set of figures illustrates the dynamic behavior of a 3D fractional-order Lorenz-like chaotic system with a fractional derivative order of $\alpha = 0.99$.

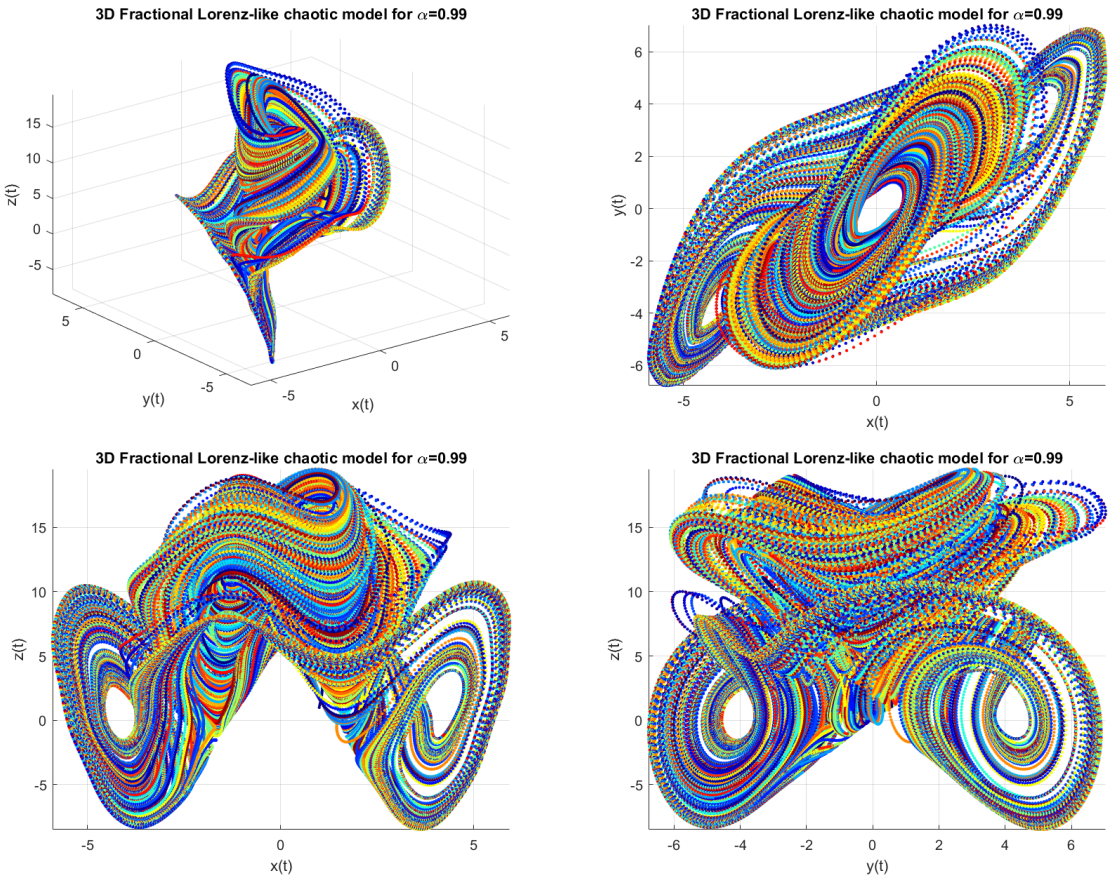

Figure 4. Phase portraits of the fractional Lorenz-like chaotic system with Caputo-Fabrizio fractional derivative.

Figure 4 shows the full 3D phase portrait of the attractor in (x, y, z) space, revealing a complex and widely structured trajectory that never intersects itself, consistent with the behavior of strange attractors. Figures three through five display 2D projections of the attractor onto the (x, y), (x, z), and (y, z) planes, respectively. The projection on the (x, y) plane resembles the well-known butterfly shape of the classical Lorenz attractor, indicating the system's similar bifurcation structure. The (x, z) and (y, z) projections further highlight the stretching and folding mechanisms that contribute to the system's sensitive dependence on initial conditions. Overall, the figures collectively demonstrate the chaotic dynamics of the fractional Lorenz-like system, shaped significantly by the memory effects introduced by the fractional-order derivative.

For $\alpha = 0.95$, we again deal with the system

$$\begin{aligned} {}_0^{CF}D_t^{\alpha} x(t) &= \sigma_1 y - \sigma x + d \sin z \\ {}_0^{CF}D_t^{\alpha} y(t) &= x(\rho - z) - y + eyz \\ {}_0^{CF}D_t^{\alpha} z(t) &= xy - \beta z + \gamma \cos x, \end{aligned} \tag{4.2}$$

which has chaotic behavior with the parameters

$$\sigma = 3,5;\ \sigma_1 = 3.9;\ \rho = 1;\ \beta = 1.1;\ d = 2.2;\ e = 0.45;\ \gamma = 31.95;$$

and the initial conditions by considering [22]

$$x(0) = 1;\ y(0) = 1;\ z(0) = 1.$$

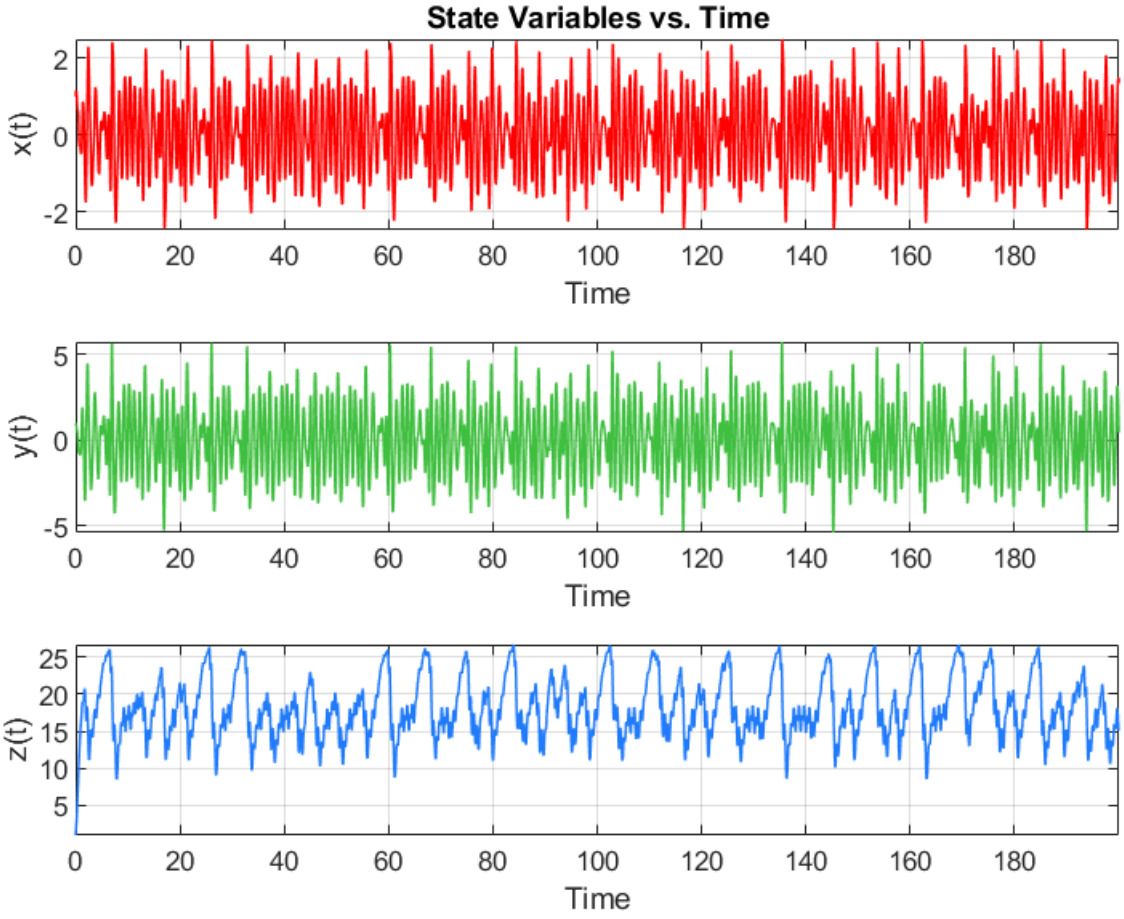

Figure 5. Simulation of the state variables $x(t), y(t)$, and $z(t)$ in a Lorenz-like chaotic system governed by the Caputo-Fabrizio fractional derivative.

Figure 5 presents time series plots of the state variables $x(t)$, $y(t)$, and $z(t)$ for a fractional-order Lorenz-like chaotic system with a fractional derivative order of $\alpha = 0.95$. The chaotic dynamics of the system are readily apparent through the irregular and non-repeating nature of the trajectories, which is a fundamental characteristic of chaotic behavior. Both $x(t)$ and $y(t)$ exhibit zero-mean oscillations, fluctuating symmetrically around the horizontal axis, while $z(t)$ displays oscillations around a positive mean value of approximately 15. Compared to $x(t)$ and $y(t)$, the variable $z(t)$ shows larger amplitude

fluctuations and a slower rate of variation, indicating distinct dynamical features among the state variables. These time series collectively illustrate the system's sensitive dependence on initial conditions, a defining property of chaos.

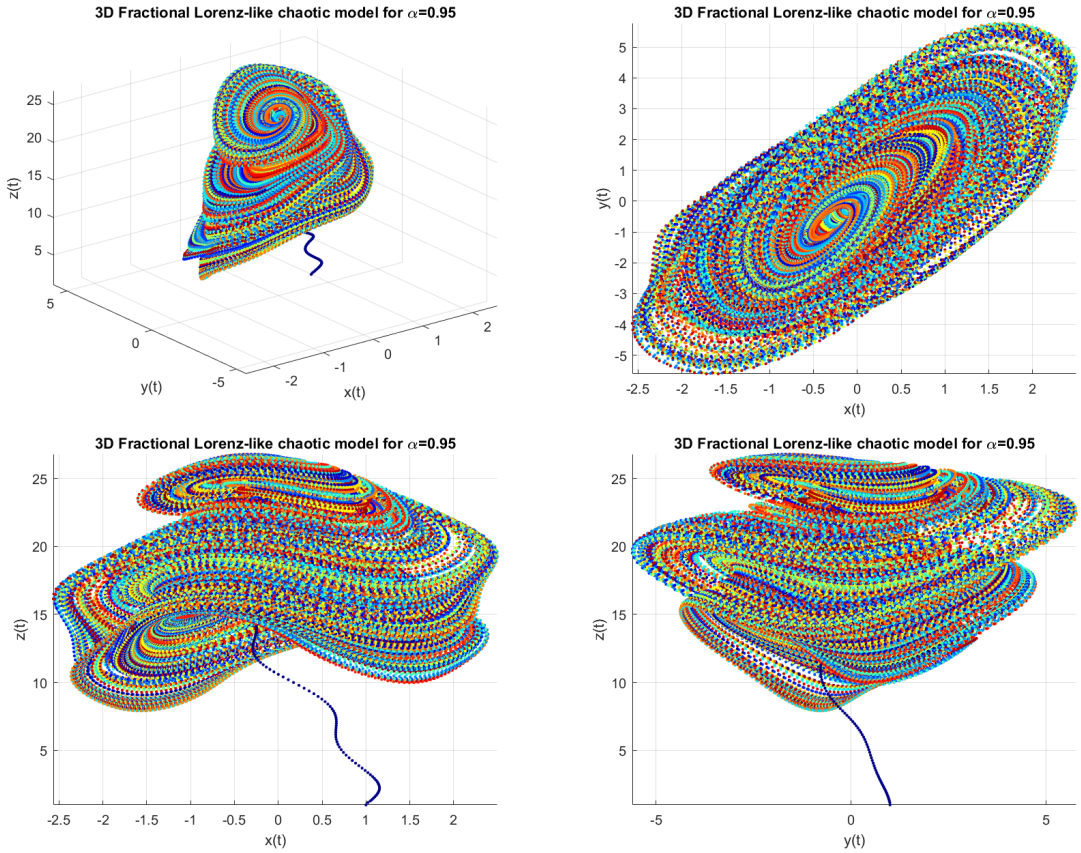

Figure 6. Phase space representations of a 3D fractional-order Lorenz-like chaotic system for $\alpha = 0.95$.

Figure 6 illustrates the phase space representations of a 3D fractional-order Lorenz-like chaotic system with a fractional derivative order of $\alpha = 0.95$. Figure 6a presents the full 3D phase portrait in $(x(t), y(t), z(t))$ space, where the trajectory forms a complex, spiraling attractor that visually resembles the classic Lorenz butterfly structure but with denser layering, highlighting the system's chaotic and memory-dependent behavior. This attractor remains bounded, yet displays sensitive dependence on initial conditions, a hallmark of chaos. Figure 6b shows the projection onto the $(x(t), y(t))$ plane, revealing elliptical and spiral structures that emphasize the intricate interaction between these two variables. The attractor's layered spirals suggest the long-term memory effect introduced by the fractional derivative. In Figure 6c, the projection $(x(t), z(t))$ reveals a stretched and layered attractor, indicating a slower variation in the z-component and more rapid fluctuations in $x(t)$. This view highlights how different variables in the system evolve on distinct time scales. Finally, Figure 6d shows the projection $(y(t), z(t))$ projection, where the attractor appears vertically extended, again confirming the slower dynamics of $z(t)$ and its nonlinear coupling with $y(t)$. Collectively, these phase space plots confirm the system's chaotic behavior and demonstrate the complexity introduced by the fractional-order dynamics.

We choose $\alpha = 0.96$ for the system

$$\begin{aligned} {}_0^C D_t^\alpha x(t) &= \sigma_1 y - \sigma x + d \sin z \\ {}_0^C D_t^\alpha y(t) &= x(\rho - z) - y + eyz \\ {}_0^C D_t^\alpha z(t) &= xy - \beta z + \gamma \cos x, \end{aligned} \tag{4.3}$$

which has chaotic behavior with the parameters

$$\sigma = 3.5;\ \sigma_1 = 4.2;\ \rho = 1;\ \beta = 0.98;\ d = 1;\ e = 0.5;\ \gamma = 25.175,$$

and the initial conditions

$$x(0) = 0;\ y(0) = 0;\ z(0) = 0.$$

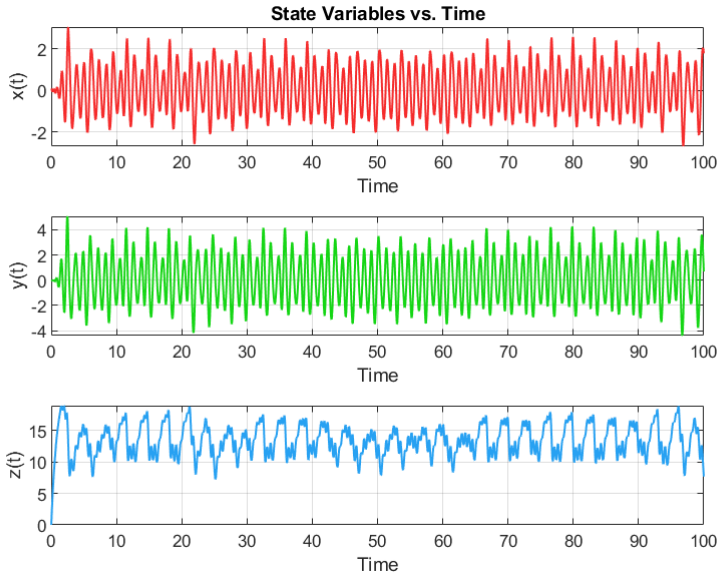

Figure 7. Time evolution of the state variables $x(t)$, $y(t)$, and $z(t)$ of the Lorenz-like chaotic system with Caputo fractional derivative.

Figure 7 shows the time evolution of the state variables $x(t)$, $y(t)$, and $z(t)$. The signals exhibit oscillatory and irregular patterns, characteristic of chaotic systems—deterministic yet highly sensitive to initial conditions. Notably, $x(t)$ and $y(t)$ oscillate with high frequency and amplitude variation, while $z(t)$ displays broader, lower-frequency oscillations, indicating differing dynamic roles among the variables.

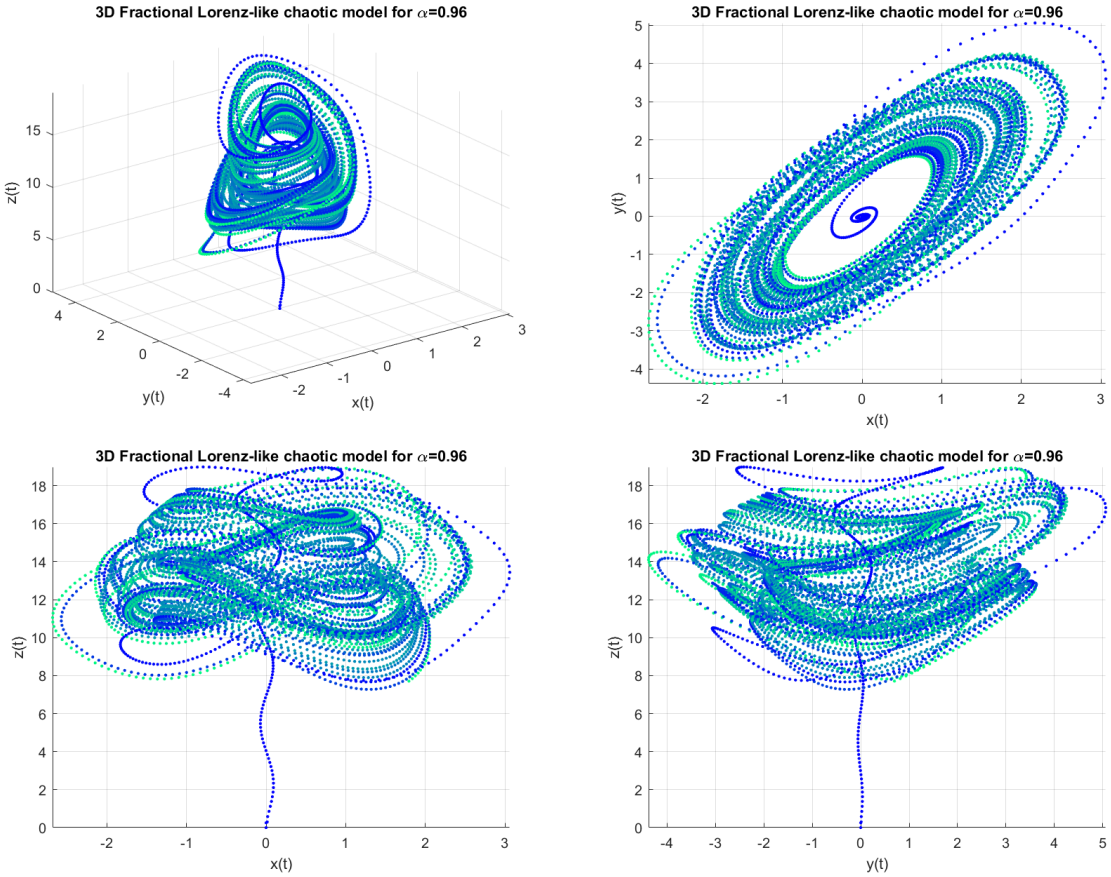

Figure 8. The behavior of a 3D fractional Lorenz-like chaotic system with a fractional order of $\alpha = 0.96$.

Figure 8 illustrates the behavior of a 3D fractional Lorenz-like chaotic system with a fractional order of $\alpha = 0.96$. Fractional-order systems generalize traditional differential equations by incorporating memory effects, which allows them to capture more complex and realistic dynamics. The subsequent phase portraits (2D and 3D) provide deeper insight into the system's chaotic attractor. The 3D plot of $x(t)$, $y(t)$, $z(t)$ shows a dense, layered, and spiral-like structure, signifying a strange attractor typical of chaotic systems. In the $x(t) - y(t)$ plane, the system forms an elliptical, closed-loop structure reminiscent of the Lorenz attractor's butterfly wings but more symmetric and densely packed. The $x(t) - z(t)$ and $y(t) - z(t)$ projections exhibit complex, intertwined trajectories, highlighting the intricate coupling and long-term memory effects induced by the fractional dynamics.

5. Conclusion and discussion

In this study, a Lorenz-like chaotic system was investigated within the framework of fractional-order differential equations. The existence and uniqueness of solutions were analyzed mathematically for different types of fractional derivatives, including Caputo–Fabrizio and Caputo. These results confirm that the system admits well-defined solutions under fractional-order dynamics. Numerical simulations were conducted for various fractional orders, and the phase portraits reveal that the chaotic behavior of the

system is preserved even when the derivative order deviates from the classical integer case. Especially for values close to 1 (e.g., $\alpha = 0.95,\ 0.99$), the system exhibits complex and chaotic dynamics, with sensitive dependence on initial conditions and intricate attractor structures.

In view of the fractional-order formulation, we now present a detailed discussion of the figures corresponding to each case. Figures 3 and 4 collectively illustrate the dynamic behavior of a fractional-order Lorenz-like chaotic system with a derivative order of $\alpha = 0.99$. The first image presents time-series plots of the state variables $x(t)$, $y(t)$, and $z(t)$, each showing oscillatory and bounded behavior, indicative of nonlinear interactions and chaotic dynamics. The 3D visualization highlights the richness of fractional-order systems, which generalize classical models by incorporating historical dependence into their dynamics. Together, these figures provide a compelling visual narrative of how fractional calculus deepens our understanding of chaotic systems, offering nuanced behavior that differs from traditional integer-order models. Figures 5 and 6 continue to explore the behavior of a fractional-order Lorenz-like chaotic system, this time with a slightly lower fractional derivative order of $\alpha = 0.95$, compared to the previous $\alpha = 0.99$. The time-series plots of $x(t)$, $y(t)$, and $z(t)$ show distinct oscillatory patterns, with $x(t)$ and $y(t)$ fluctuating rapidly within a narrow range, while $z(t)$ exhibits broader, more irregular swings between 10 and 30. This suggests that the system's vertical dynamics (represented by $z(t)$) are more volatile, possibly due to nonlinear amplification or coupling effects. The 3D visualization further enriches this understanding, showing a swirling, multicolored attractor in full dimensionality—$x(t)$, $y(t)$, and $z(t)$—where the chaotic nature is vividly captured through its non-repeating, intricate loops. The use of fractional calculus with $\alpha = 0.95$ introduces memory effects that make the system's evolution dependent not only on its current state but also on its past, resulting in richer and more nuanced dynamics than traditional integer-order models. Figures 7 and 8 collectively offer a compelling visualization of a fractional-order Lorenz-like chaotic system, highlighting both its temporal evolution and spatial complexity. Figure 7 presents time-series plots of three state variables—$x(t)$, $y(t)$, and $z(t)$—revealing distinct dynamic behaviors. Both $x(t)$ and $y(t)$ exhibit high-frequency oscillations with similar amplitude ranges, suggesting tightly coupled or symmetric dynamics, while $z(t)$ displays a more irregular and less periodic pattern, possibly reflecting its role as an integrative or slower-evolving variable within the system. 3D visualization showcase the system's trajectory in three-dimensional space for a fractional order of $\alpha = 0.95$, forming intricate, looping structures characteristic of chaotic attractors. The use of fractional calculus introduces memory effects, enriching the system's behavior beyond classical models and making it more representative of real-world phenomena. Together, these visualizations underscore the sensitivity, complexity, and unpredictability inherent in fractional-order chaotic systems, offering valuable insights for studies in nonlinear dynamics, control theory, and applied physics.

The results demonstrate that fractional-order modeling provides an effective approach for exploring the memory and hereditary properties of chaotic systems. Compared to the classical model, the fractional version offers greater flexibility in capturing nuanced behaviors and transitions in the system's dynamics. This highlights the potential of fractional calculus in enriching the theoretical understanding and simulation of chaotic systems.

Author contributions

Seda İĞRET ARAZ: conceptualization, investigation, methodology, software, supervision, visualization, writing-review and editing; Mehmet Akif ÇETİN: conceptualization, investigation, methodology, software, visualization, writing-review and editing.

Use of Generative-AI tools declaration

The authors declare they have not used Artificial Intelligence (AI) tools in the creation of this article.

Acknowledgements

The authors would like to thank the anonymous reviewers for carefully reading the paper and providing valuable comments.

Conflict of interest

On behalf of all authors, the corresponding author states that there are no funding and/or conflicts of interests/conflict of interest.

References

1. E. N. Lorenz, Deterministic nonperiodic flow, *J. Atmos. Sci.*, **20** (1963), 130–141.
2. C. Sparrow, *The Lorenz equations: Bifurcations, chaos, and strange attractors*, New York: Springer-Verlag, 1982. https://doi.org/10.1007/978-1-4612-5767-7
3. G. Chen, T. Ueta, Yet another chaotic attractor, *Int. J. Bifurcation Chaos*, **9** (1999), 1465–1466. https://doi.org/10.1142/S0218127499001024
4. J. Lü, G. Chen, D. Cheng, A new chaotic attractor coined, *Int. J. Bifurcation Chaos*, **12** (2002), 659–661. https://doi.org/10.1142/S0218127402004620
5. C. Li, G. Chen, Chaos in the fractional order Chen system and its control, *Chaos Solitons Fractals*, **22** (2004), 549–554. https://doi.org/10.1016/j.chaos.2004.02.035
6. I. Petráš, *Fractional-order nonlinear systems: Modeling, analysis and simulation*, Berlin: Springer-Verlag, 2011. https://doi.org/10.1007/978-3-642-18101-6
7. M. S. Tavazoei, M. Haeri, A proof for nonexistence of chaos in linear fractional-order systems, *Automatica*, **43** (2007), 918–920. https://doi.org/10.1016/j.automatica.2009.04.001
8. Z. M. Odibat, N. Corson, M. A. Aziz-Alaooi, C. Bertelle, Synchronization of chaotic fractional order systems via linear control, *Int. J. Bifurcation Chaos*, **20** (2010), 81–97. https://doi.org/10.1142/S0218127410025429
9. S. Boulaaras, S. Arunachalam, S. Sriramulu, Results on Ulam–Hyers stability of nonlinear Chen system with fractional-order derivative, *Asian J. Control*, 2025, 1–14. https://doi.org/10.1002/asjc.3656
10. I. Akbulut Arık, S. Igret Araz, Delay differential equations with fractional differential operators: Existence, uniqueness and applications to chaos, *Commun. Anal. Mech.*, **16** (2024), 169–192. https://doi.org/10.3934/cam.2024008
11. K. A. Abro, A. Atangana, J. F. Gomez-Aguilar, Chaos control and characterization of brushless DC motor via integral and differential fractal-fractional techniques, *Int. J. Model Simul.*, **43** (2022), 416–425. https://doi.org/10.1080/02286203.2022.2086743

12. M. Sinan, J. Leng, K. Shah, T. Abdeljawad, Advances in numerical simulation with a clustering method based on K–means algorithm and Adams Bashforth scheme for fractional order laser chaotic system, *Alex. Eng. J.*, **75** (2023), 165–179. https://doi.org/10.1016/j.aej.2023.05.080
13. I. Haq, N. Ali, H. Ahmad, Analysis of a chaotic system using fractal-fractional derivatives with exponential decay type kernels, *Math. Model. Control*, **2** (2022), 185–199. https://doi.org/10.3934/mmc.2022019
14. X. Zhang, B. Sang, B. Li, J. Liu, L. Fan, N. Wang, Hidden chaotic mechanisms for a family of chameleon systems, *Math. Model. Control*, **3** (2023), 400–415. https://doi.org/10.3934/mmc.2023032
15. S. Igret Araz, M. B. Riaz, Qualitative behavior and bifurcation structure of a new Lorenz-type chaotic model, preprint, hal-05175933.
16. M. Caputo, M. Fabrizio, A new definition of fractional derivative without singular kernel, *Progr. Fract. Differ. Appl.*, **1** (2015), 73–85.
17. M. Caputo, Linear model of dissipation whose Q is almost frequency independent II, *Geophys. J. Int.*, **13** (1967), 529–539. https://doi.org/10.1111/j.1365-246X.1967.tb02303.x
18. A. Wolf, J. B. Swift, H. L. Swinney, J. A. Vastano, Determining Lyapunov exponents from a time series, *Physica D*, **16** (1985), 285–317. https://doi.org/10.1016/0167-2789(85)90011-9
19. J. Kaplan, J. Yorke, Chaotic behavior of multidimensional difference equations, In: *Functional Differential Equations and the Approximation of Fixed Points,* Berlin: Springer, 1979. https://doi.org/10.1007/BFb0064319
20. A. Atangana, S. Igret Araz, Step forward on nonlinear differential equations with the Atangana-Baleanu derivative: Inequalities, existence, uniqueness and method, *Chaos Solitons Fractals*, **173** (2023). https://doi.org/10.1016/j.chaos.2023.113700
21. M. Toufik, A. Atangana, New numerical approximation of fractional derivative with non-local and non-singular kernel: Application to chaotic models, *Eur. Phys. J. Plus*, **132** (2017), 444. https://doi.org/10.1140/epjp/i2017-11717-0
22. K. Dielthem, R. Garrappa, A. Giusti, M. Stynes, Why fractional derivatives with nonsingular kernels should not be used, *Fract. Calc. Appl. Anal.*, **23** (2010), 610–634. https://doi.org/10.1515/fca-2020-0032
23. V. Daftardar-Gejji, H. Jafari, An iterative method for solving nonlinear functional equations, *J. Math. Anal. Appl.*, **316** (2006), 753–763. https://doi.org/10.1016/j.jmaa.2005.05.009
24. S. M. Sivalingam,V. Govindaraj, J. V. C. Sousa, A. S. Hendy, L1-predictor–corrector method for ψ-Caputo type fractional differential equations, *Comput. Appl. Math.*, **44** (2025), 753–763. https://doi.org/10.1007/s40314-025-03192-0

AIMS Press